Benchmarking density functional perturbation theory to enable high-throughput screening of materials for dielectric constant and refractive index

Ioannis Petousis, Wei Chen, Geoffroy Hautier, Tanja Graf, Thomas D. Schladt, Kristin A. Persson, and Fritz B. Prinz

Phys. Rev. B **93**, 115151 — Published 31 March 2016

DOI: 10.1103/PhysRevB.93.115151

Benchmarking of the Density Functional Perturbation Theory to enable the high-throughput screening of materials for the dielectric constant and refractive index

Ioannis Petousis,[1] Wei Chen,[2,3] Geoffroy Hautier,[4] Tanja Graf,[5]
Thomas D. Schladt,[5] Kristin Persson,[6] and Fritz B. Prinz[1,7]

[1]*Department of Materials Science and Engineering, Stanford University, Stanford, CA 94305, USA*
[2]*Energy Technologies Area, Lawrence Berkeley National Laboratory, Berkeley, CA 94720, USA*
[3]*Department of Mechanical, Materials and Aerospace Engineering, Illinois Institute of Technology, Chicago, IL 60616, USA*
[4]*Institute of Condensed Matter and Nanosciences, Université catholique de Louvain, 1348 Louvain-la-Neuve, Belgium*
[5]*Volkswagen Group Research, Berliner Ring 2, 38840 Wolfsburg, Germany*
[6]*Department of Materials Science and Engineering, Hearst Mining Memorial Building, Berkeley, CA 94720, USA*
[7]*Department of Mechanical Engineering, Stanford University, Stanford, CA 94305, USA*

We demonstrate a high-throughput Density Functional Perturbation Theory (DFPT) methodology capable of screening compounds for their dielectric properties. The electronic and ionic dielectric tensors are calculated for 88 compounds, where the eigenvalues of the total dielectric tensors are compared with single crystal and polycrystalline experimental values reported in the literature. We find that GGA/PBE has a smaller mean average deviation from experiments (MARD=16.2%) when compared to LDA. The prediction accuracy of DFPT is lowest for compounds that exhibit complex structural relaxation effects (e.g. octahedra rotation in perovskites) and/or strong anharmonicity. Despite some discrepancies between DFPT results and reported experimental values, the high-throughput methodology is found to be useful in identifying interesting compounds by ranking. This is demonstrated by the high Spearman correlation factor ($\rho = 0.92$). Finally, we demonstrate that DFPT provides a good estimate for the refractive index of a compound without calculating the frequency dependence of the dielectric matrix (MARD=5.7%).

I. INTRODUCTION

Dielectric materials form an integral component of electronic devices such as capacitors and field effect transistors and hence, are particularly important for a plethora of modern technologies, from computer memory (DRAM) to sensors and communication circuits. Furthermore, supercapacitors can be attractive for energy storage due to their fast charge and discharge performances. Another quantity that results from the electronic part of the dielectric constant is the refractive index. A material's refractive index is a critical property for optical applications such as light-emitting diodes and optical fibers with applications that extend from communications and electronics to the automotive industry.

Improved dielectric materials would not only allow for cheaper and more efficient devices but could also help in miniaturization. There is a need for materials with specific dielectric properties, both low-k and high-k. Given the trend towards all-electric vehicles, the transportation sector is likely to become increasingly involved in the search for optimal dielectric and optical materials with requirements that might be quite different to those of the electronics industry. High-throughput *ab initio* simulations that can calculate properties for thousands of materials[1] would tremendously accelerate the field of dielectric materials design. Over the last few years there have been efforts to perform high-throughput *ab initio* calculations in order to accelerate materials discovery and to create databases focusing, for example, on band gap and structure prediction[2–5]. In the case of dielectric materials, Density Functional Perturbation Theory[6,7] (DFPT) provides a relatively inexpensive way to compute both the electronic and ionic tensors.

In this article, we focus on high-throughput screening specifically tailored to the discovery of new dielectric materials[8,9]. The first step is to carefully assess the accuracy of the method and the cases where it can, (or cannot), be applied. We propose and assert a high-throughput methodology for dielectric tensor computations within DFPT, testing convergence parameters on a set of 88 known compounds, where we compare the results to experimental data. In this way, we obtain a large scale and statistically significant assessment of the typical error from DFPT within both the Local Density Approximation[10] (LDA) and the Generalized Gradient Approximation[11,12] (GGA). In particular, we compare all 88 compounds - consisting of 42 elements and belonging to 14 point groups - with experimental data by benchmarking against the eigenvalues of dielectric tensors of single crystals when that information is available. This work is, to the best of our knowledge, the largest comparison of DFPT results with experimental data for both the dielectric constant and refractive index.

II. THEORY AND METHODOLOGY

In order to validate the high-throughput workflow, the computational results were benchmarked against 88

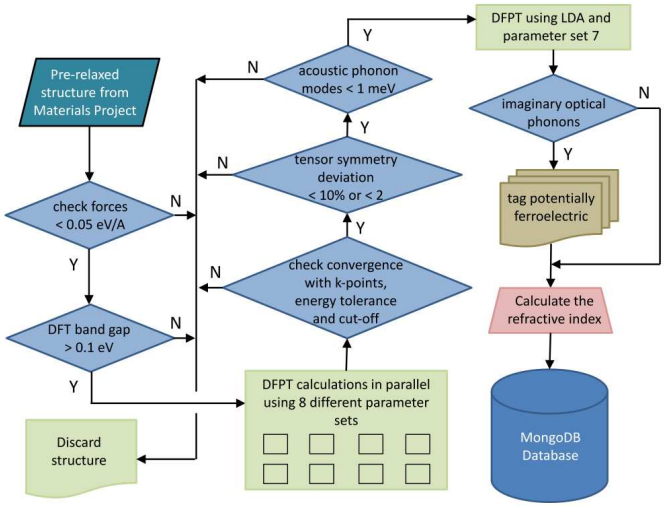

FIG. 1. Flowchart summarizing the methodology for calculating the dielectric constant of compounds using DFPT.

compound structures, for which experimental measurements were found. The calculation methodology is summarized in the flowchart in figure 1. All structures were downloaded from the Materials Project Database[2,3]. To ensure adequate structure relaxation and suitability, they were checked to have interatomic forces less than 0.05 eV/Angstrom and a bandgap higher than 0.1 eV. It should be noted that the compounds in the Materials Project Database are calculated with GGA/GGA+U[11–13], which would likely underestimate the band gap. However, there are also cases for which a more careful calculation yields a metal[14]. Using the DFPT method as implemented in the Vienna Ab-initio Simulation Package (VASP)[15–18] the dielectric constant was calculated using 8 different parameter sets (table I). For all calculations, the Projector Augmented Wave (PAW) pseudopotentials[19,20] and the GGA/PBE[11,12] +U[13,14] exchange-correlation functional were used. In each simulation the electronic convergence was assumed successful once the energy change was less than the predefined energy tolerance (see table I). In addition, using parameter set 7 from table I, we performed calculations with the LDA[10] exchange-correlation functional, for comparison with GGA.

The total dielectric tensor ϵ_{total} is given by:

$$\epsilon_{total} = \epsilon_\infty + \sum_\mu \epsilon_\mu \tag{1}$$

where ϵ_∞ is the electronic contribution and ϵ_μ is the oscillator strength for mode μ. The ionic contribution is included by perturbing the structure along certain directions and calculating the resulting polarization. The

TABLE I. Parameters for the 8 different calculation sets and the average required CPU time. A k-point density of 1,000 implies a k-point mesh of 1,000 / (number of atoms in supercell). The quoted CPU times are total, across all cores. We used 24 cores for each calculation.

	Set 1	Set 2	Set 3	Set 4	Set 5	Set 6	Set 7	Set 8
k-point density	1000	3000	6000	9000	3000	3000	3000	3000
Energy tolerance (eV)	10^{-6}	10^{-6}	10^{-6}	10^{-6}	10^{-5}	10^{-7}	10^{-6}	10^{-6}
Energy cut-off (eV)	800	800	800	800	800	800	600	1000
Average CPU time (hours)	350	416	480	589	337	447	349	429

Born effective charge for ion α is defined as:

$$Z^*_{\alpha,ij} = \frac{\Omega}{|e|}\frac{\partial P_i}{\partial r_j^{(\alpha)}} \tag{2}$$

where e is the electronic charge, Ω the supercell volume, P_i the polarization in direction i and $r_j^{(\alpha)}$ the position in space of ion α in coordinate j.

The oscillator strength for each phonon mode μ can be calculated using:

$$\epsilon_\mu = \sum_{\alpha\beta ijk} \frac{Z^*_{\alpha,ij} Z^*_{\beta,ik} a_{\mu,\alpha j} a_{\mu,\beta k}}{3 m_\alpha^{1/2} m_\beta^{1/2} \Omega \epsilon_0 \omega_\mu^2} \tag{3}$$

where m_α is the mass of ion α and ϵ_0 the permittivity of free space. a_μ and ω_μ are the eigen-mode and eigen-frequency of mode μ which are determined with the help of the force-constant tensor (Hessian of the energy with respect to ionic positions). More details about how the electronic dielectric tensor, Born effective charges, force-constant matrix and the related dynamical matrix are calculated within the framework of DFPT are given in the following references[7,21–23].

Regarding the calculation of ϵ_∞ we note that local field effects are sometimes not included, which is specified in the surrounding text. The term "local field effects" signifies how the microscopic dielectric tensor is being inverted. Formally, the macroscopic dielectric tensor is calculated from its microscopic analogue as:

$$\epsilon_{\text{mac}} = \frac{1}{\left(\epsilon_{\text{mic}}^{-1}\right)_{\mathbf{G}=\mathbf{0},\mathbf{G}'=\mathbf{0}}} \tag{4}$$

where and $\mathbf{G}$ and $\mathbf{G}'$ are reciprocal lattice vectors. If we assume ϵ_{mic}^{-1} to be quasi-diagonal, we ignore local field effects and the above formula becomes:

$$\epsilon_{\text{mac}} = \left(\epsilon_{\text{mic}}\right)_{\mathbf{G}=\mathbf{0},\mathbf{G}'=\mathbf{0}} \tag{5}$$

After each DFPT calculation, a number of sanity checks were implemented (figure 1). First, the calculated dielectric tensor was ensured to be symmetric and to have the right structure for the point group of the compound. Specifically, it was checked that the change in the dielectric tensor by symmetry operations in the respective point group was less than 10% or 2 relative and absolute respectively. In addition, materials with a Gamma point acoustic phonon mode greater than 1 meV were excluded. However, compounds with imaginary optical Brillouin Zone phonon modes were flagged as potentially ferroelectric.

In order to validate the computational results, the eigenvalues of the dielectric tensor were compared directly with those obtained experimentally. If experimental results on single crystals were not available, an effective polycrystalline dielectric constant was calculated according to[24]:

$$\epsilon_{poly} = \frac{3\lambda_1\lambda_2\lambda_3}{\lambda_1\lambda_2 + \lambda_1\lambda_3 + \lambda_2\lambda_3} \tag{6}$$

where λ_i are the eigenvalues of the calculated dielectric tensor. The experimental values were all measured at room temperature - except for a few cases where the temperature was not specified.

The refractive index is calculated by taking the square root of the average of the eigenvalues of the electronic dielectric tensor. Here we assume that the ions do not relax in the external electric field at optical frequencies and hence the ionic contribution to the dielectric constant is negligible.

Finally, in order to quantify the deviation of DFPT results from experimental values, we define the Mean Absolute Relative Deviation (MARD) as:

$$MARD(x) = \frac{100}{N}\sum_{i=1}^{N}\frac{|x_i - \overline{x}_i|}{\overline{x}_i} \tag{7}$$

where N is the number of compounds, x the DFPT calculated value and $\overline{x}$ the experimental value.

III. CONVERGENCE

Figure 2 shows the convergence of the electronic and ionic tensors with k-point density, energy tolerance and energy cut-off. From the scale of the y-axis, it is immediately apparent that the electronic tensor converges faster with energy tolerance and energy cut-off than the ionic part. Conversely, the number of k-points appears to be important for both.

We believe the ionic portion converges slower than the electronic due to the extra calculation steps required to obtain the phonon eigenfrequencies and eigenmodes. In order to calculate the ionic contribution, it is necessary to obtain in addition to the converged electronic structure, a converged force-constant matrix which depends on the Hessian of both electron-ion and ion-ion interactions. Indeed, we observed that most materials with equal or higher than 10% convergence error in the electronic tensor, have equal or higher than 10% error in the ionic tensor too.

More specifically, regarding convergence of the electronic tensor, we found the materials that had equal or higher than 10% convergence error at a k-point density of 1,000 were: CuCl, CuBr, ZnO, CdSe, PbS and PbSe. Interestingly, these are all direct band gap materials with relatively low DFT energy gap and high band curvature at the band gap. Hence, one should expect that a denser k-point mesh would be required to model electronic transitions between bands. The materials with equal or higher than 10% error in the ionic tensor at a k-point density of 1,000 were: CuCl, CuBr, PbS, PbSe and $AlCuSe_2$. This result corroborates the propagation of errors from the electronic to the ionic constant as argued in the previous paragraph. In the case of $AlCuSe_2$, we note that the convergence difficulty may be ionic in origin due to the relatively large unit cell (8 atoms) and the low symmetry group ($I\overline{4}2d$). Interestingly, $AlCuSe_2$ exhibits an error $> 10\%$ in the ionic tensor even at a k-point density of 3,000.

Table I lists the average CPU time for the different parameter sets. Since this is a screening workflow, computational efficiency is of paramount importance in order to allow scanning of a large number of compounds. By comparing figure 2 with table I, we believe that parameter set 7 is a good balance between efficiency and computational convergence and hence, was chosen for comparison of DFPT results with experimental data. Between different compounds, we found that a significant part of the total CPU time is devoted to the calculation of the ionic part of the dielectric tensor. As a result, unit cells with relatively more atomic sites and degrees of freedom are computationally more expensive.

For electronic convergence, a combination of the blocked Davidson iteration scheme and RMM-DIIS algorithms were used for speed. However, difficult-to-converge cases necessitated the exclusive use of the more robust blocked Davidson iteration scheme. Our code performs the change automatically if electronic convergence is not achieved.

The results of the suggested workflow can, in most cases, be assumed to be the converged DFPT values within $\pm 10\%$. However, since this is a screening methodology, once an interesting material has been identified, it is still recommended to run additional calculations with parameters specifically tailored to the individual compound.

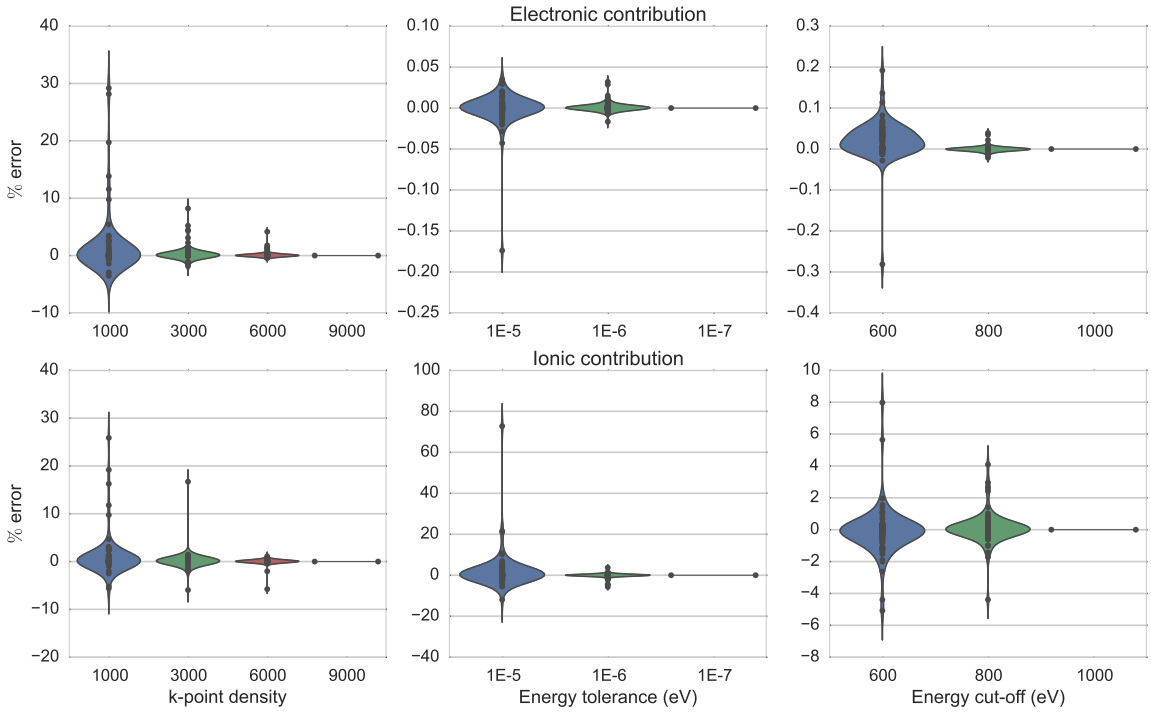

FIG. 2. Violin plot showing convergence of the electronic (top) and ionic (bottom) contributions with different simulation parameters. The violin outline is the gaussian kernel density estimate of the data points that appear in the middle. Reference calculations are rightmost on each sub-plot and appear as a horizontal line.

IV. COMPARISON WITH EXPERIMENTAL DATA AND BENCHMARKING

In figure 3, we see that in most cases, it is possible to predict the dielectric constant of materials with a relative deviation of less than +/- 25% from experimental values at room temperature. Including local field effects gives the smallest mean absolute relative deviation (MARD=16.2% for GGA). The MARD for LDA is larger, 20.4%, therefore the following discussion refers to GGA results unless explicitly stated. Furthermore, we note a tendency to overestimate rather than underestimate the dielectric constant relative to experiments, which is a well-known effect of DFPT[25–27] for the electronic contribution. Although it has often been related to the band gap underestimation problem of DFT, DFPT is a ground state theory and hence, the dielectric constant should, in principle, be described exactly[26]. In fact, as described by various authors, the problem is likely linked to the exchange-correlation functional[26,28–32]. Specifically, the exchange correlation functional has been found to depend on polarization but the actual dependence formula is, unfortunately, not known[26,29,30]. Additionally, the validity of GGA depends on the charge density varying slowly - an assumption that may be broken when an external electric field is applied[28].

There are several reasons why one should not expect exact agreement between experimental results and DFPT. First of all, DFPT results should be compared to those of a single crystal which, are often not available. Although, in such cases, equation 6 was used, it should be kept in mind that it is only an approximation oblivious to the size or directionality of the grains. Furthermore, several other aspects, not included here, can affect the experimental results, e.g., (1) temperature, (2) pressure[33], (3) impurities, vacancies and defects in general, (4) interfaces and (5) surface charges. For example, temperature can impact the dielectric constant both negatively and positively[34]. Most importantly, experimental results can vary significantly for the same compound and depend on, for example, how the crystal was prepared, the grain size and measurement technique. For instance, for SnS_2 at T=300K, Lucovsky *et al.*[35] found a value of 17.7 using Kramers Kronig analysis of IR-spectra while Nikolic *et al.*[36] reported a value of 20.25 from the interference fringes in transmission measurements, constituting a 7% deviation from the mean. $SrTiO_3$ has a dielectric constant of ∼300 at room temperature but it increases to ∼30,000 close to 0 K[37]. Another example is that of $BaTiO_3$ for which, depending on the synthesis technique, dielectric constant values ranging from 500 to 6,900 have been reported[38].

From figure 3, we find that specifically Te, $AlCuSe_2$ (un-converged) and MgF_2, appear as outliers. $AlCuSe_2$ has the chalcopyrite crystal structure in which anharmonic effects have been shown to be important[39]. As discussed below in more detail, anharmonic effects may lead to over- as well as under-estimation of the dielectric

TABLE II. List of perovskites, thallous halides and lead chalcogenides. MP ID is the Materials Project Database[2,3] ID number for each compound.

Compound	MP ID	Spacegroup	ϵ_{total}^{GGA}	ϵ_{total}^{LDA}	$\epsilon_{experimental}$
$BaTiO_3$	mp-5986	P4mm	19.44	39.5	2445[44]
$SrTiO_3$	mp-5229	$Pm\overline{3}m$	8.63	249.65	300[44]
$BaZrO_3$	mp-3834	$Pm\overline{3}m$	73.02	55.2	43[45]
$KNbO_3$	mp-5246	C2mm	24.04	71.1	890[44]
$LiNbO_3$	mp-3731	R3c	41.22	45.3	64.55[44]
TlCl	mp-23167	Pm-3m	232.83	44.7	32.7[46]
TlBr	mp-22875	Pm-3m	180.17	40.8	30.6[47]
TlI	mp-23197	Pm-3m	154.71	44.5	29.6[48]
PbS	mp-21276	Fm-3m	284.25	140.0	169[49]
PbSe	mp-2201	Fm-3m	364.75	151.6	210[50]
PbTe	mp-19717	Fm-3m	335.37	181.1	414[51]

constant. It is also interesting that, with the exception of MgF_2, all other outliers (including the LDA ones) are chalcogenide compounds.

We also note that some perovskite compounds (except for $LiTaO_3$), thallous halides and lead chalcogenides have been excluded from figure 3, but are listed separately in table II. These compounds are ferroelectric or paraelectric with a significant ionic contribution component. Perovskite structures also present a relaxation challenge due to the octahedral rotation effect[33,41,42] that is difficult to capture with a single unit cell. However, it should be mentioned that the high-throughput GGA results reported here agree well with other, *compound-bespoke*, *ab-initio* calculations for the electronic component of the dielectric constant (ϵ_∞) and Born effective charges (Z^*) (table III).

Comparing the GGA to the LDA results in table II we observe that the latter performs significantly better for certain compounds (especially for the thallous halides, $SrTiO_3$ and $BaZrO_3$). However, as others authors have found, the agreement may be fortuitous[37] and possibly attributed to cancellation of errors[43]. For example, from table II we observe that even though the LDA dielectric constant of $SrTiO_3$ appears to be relatively close to the experimental value at room temperature, this agreement becomes questionable if one considers the experimental value at 0 K which is ∼30,000[37]. It is also interesting that for $SrTiO_3$, including $3s$ and $3p$ valence electrons in the Ti pseudopotential, we found that the LDA result changes from 249.65 in table II to 626.10. The respective change using GGA was 8.70 to 8.29.

Ferroelectrics, thallous halides, PbS, PbSe and PbTe have been shown to exhibit significant anharmonic phonon modes[56–60] while DFPT assumes quasi-harmonic modes. Szigeti[61] defined a parameter G that represents the anharmonic contribution to the dielectric constant:

$$G = T\left[\left(\frac{\partial \epsilon_{total}}{\partial T}\right)_V - \left(\frac{\partial \epsilon_\infty}{\partial T}\right)_V\right] \tag{8}$$

In their study of TlCl and TlBr, Shanker and Sundaraj[58] estimated large negative values for G and a large negative dependence of the dielectric constant on temperature. So, it is likely that many of the aforementioned effects like temperature and pressure combine with anharmonic behavior to produce the values in table II. Interestingly, we note that the value for $LiTaO_3$ (c.f. figure 3) is within the +/-25% deviation boundaries even though it is a ferroelectric perovskite (space group: R3c) that exhibits strong anharmonicity. However, mode softening for $LiTaO_3$ occurs at approximately 500 K[62]. Hence, we do not expect $LiTaO_3$ to exhibit strong anharmonic effects at room temperature i.e. the temperature at which the dielectric constant was measured experimentally. Furhermore, for $BaTiO_3$, $SrTiO_3$ and $KNbO_3$ we found imaginary optical phonon modes at the Gamma point. Flagging these 3 compounds as ferroelectric is indeed corroborated by experiments since they are widely known to exhibit such behavior.

Despite these inherent weaknesses, it is possible to identify compounds with suitable dielectric properties if one considers the ranking or relative dielectric constant. Figure 4 shows that the ranking of the compounds based on the DFPT prediction relative to that from experimental values yields a Spearman correlation factor of 0.92. The Spearman correlation factor is defined as[63]:

$$\rho = 1 - \frac{6}{n(n^2-1)}\sum_i (x_i - y_i)^2 \tag{9}$$

where x and y contain the ranking of each element of 2 series X and Y and n is the number of elements in each of X and Y. It takes a maximum value of 1 when the rankings of series X and Y are exactly the same. The high Spearman correlation factor has important implications as it provides a high-throughput tool to identify promising compounds that can be selected for in-depth studies. After the high-throughput screening, one could further analyze the materials that lie in the range of interest to further understand their response to external electric fields.

V. REFRACTIVE INDEX

Figure 5 shows the comparison of the predicted refractive index with the experimental values for a subset of 85 compounds. The MARD and Spearman correlation factor were calculated as 5.7% and 0.96 respectively. In order to compare our calculated values, the experimental refractive index for each compound was obtained directly from the literature. Since the refractive index is

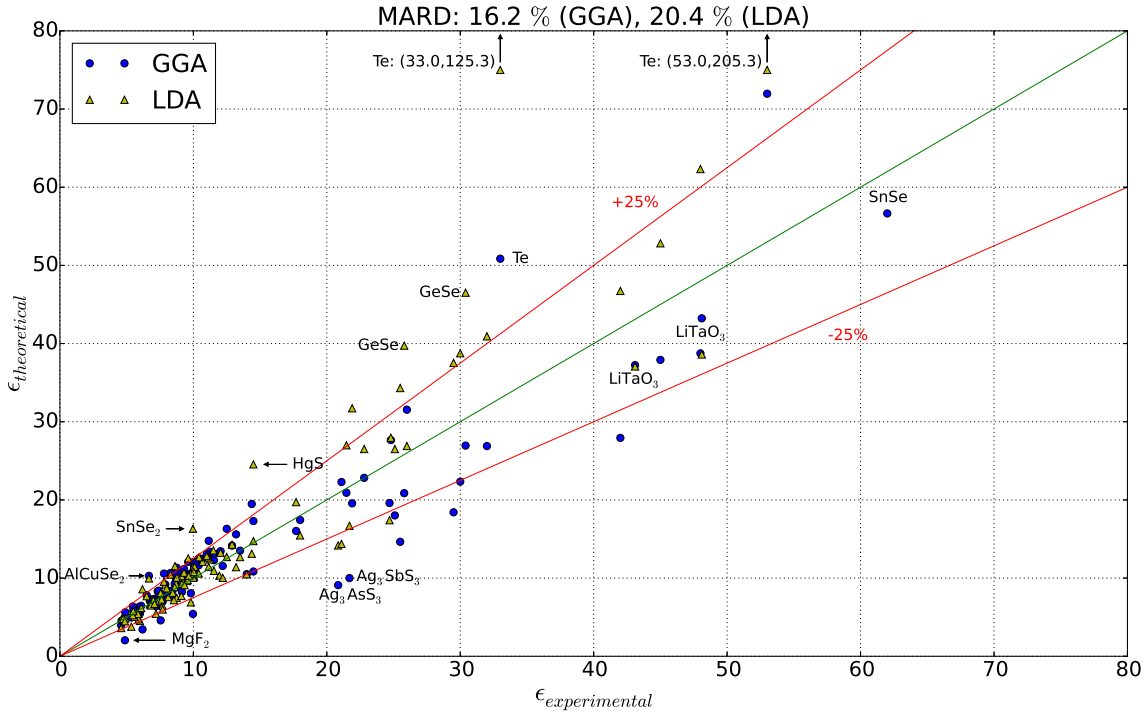

FIG. 3. DFPT prediction versus experimental values[40]. The eigenvalues of the dielectric tensor are compared directly when available experimentally as described in the theory section. Outliers with a deviation larger than 50% relative to experiments have been highlighted. $LaTiO_3$ and SnSe have also been highlighted for information.

TABLE III. Comparison of some compounds from table II with other, *compound-bespoke*, *ab-initio* studies.

Compound	ϵ_∞	ϵ_∞ (other studies)	Z^*	Z^* (other studies)
$BaTiO_3$	6.3	5.6 [a][52]	Ba:2.69, Ti:6.95, $O_\parallel$:-5.63, $O_\perp$:-2.10	Ba:2.77, Ti:7.25, $O_\parallel$:-5.71, $O_\perp$:-2.15 [a][52]
$SrTiO_3$	6.4	6.63[53]	Sr:2.55, Ti:7.45, $O_\parallel$:-5.94, $O_\perp$:-2.03	Sr:2.55, Ti:7.56, $O_\parallel$:-5.92, $O_\perp$:-2.12[53]
$BaZrO_3$	5.0	4.91[54]	Ba:2.72, Zr:6.23, $O_\parallel$:-4.95, $O_\perp$:-2.00	Ba:2.75, Zr:6.12, $O_\parallel$:-4.8, $O_\perp$:-2.03[54]
TlCl	5.0	-	1.98	2.02[55]
TlBr	5.7	5.2[55]	2.06	2.10[55]
TlI	6.6	-	2.17	2.21[55]
PbS	15.8	16.42[56]	4.4	4.4[56]
PbSe	19.8	19.23[56]	4.8	4.9[56]
PbTe	26.5	25.26[56]	5.7	6.5[56]

[a] for a cubic structure

a function of frequency, we chose to record the value at, or close to, 590nm given that the index was also measured at that wavelength and that the compound was reasonably far from resonance. For directional crystals, we calculated a simple average of the different directions, which is justified given that the current analysis is oblivious to frequency effects. The systematic overestimation of the electronic part of the dielectric constant discussed in the previous section becomes more apparent in figure 5. Table IV shows that neglecting the local field effects increases the MARD by approximately 23%. The mean absolute relative deviation is lower than that for the dielectric constant and less than half as one might have expected from the square root relationship. The latter stems from the fact that the deviation of the DFPT prediction from experiments is smaller for the electronic contribution than for the ionic. Overall, figure 5 shows that a reasonably good estimate for the refractive index can be obtained from static DFPT calculations that consider no frequency or resonance effects.

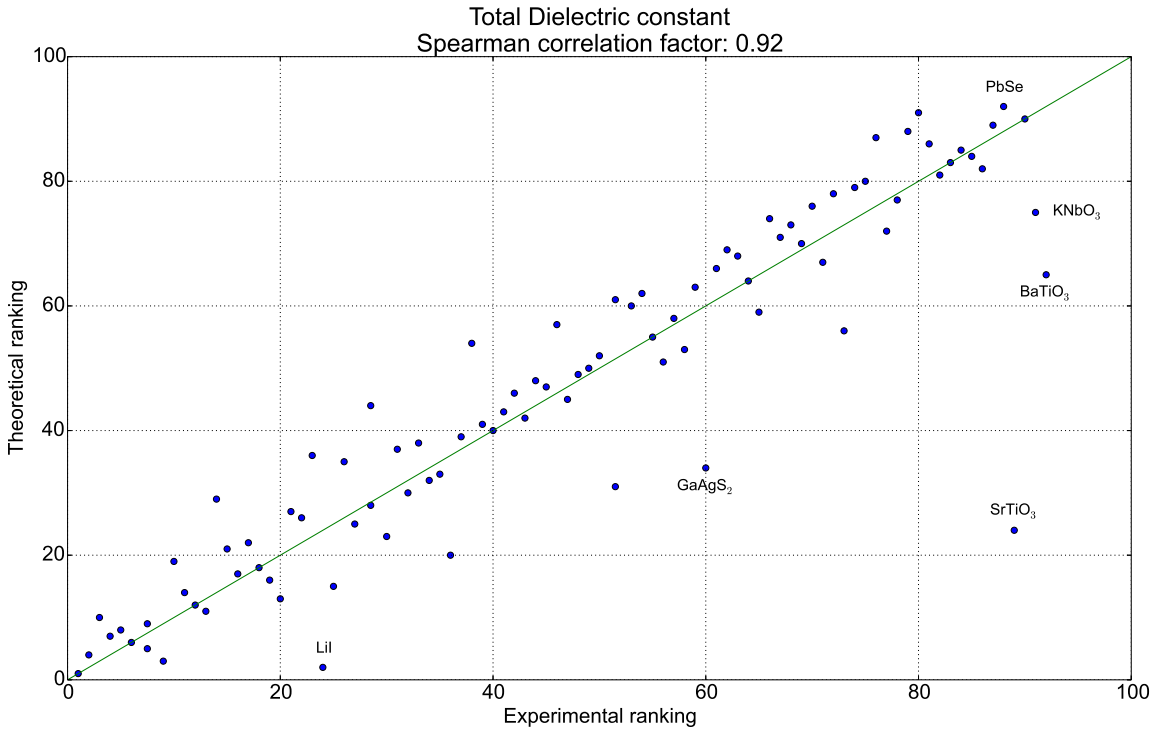

FIG. 4. Theoretical ranking of dielectric constant of materials versus the experimental ranking. The Spearman correlation factor is 0.92.

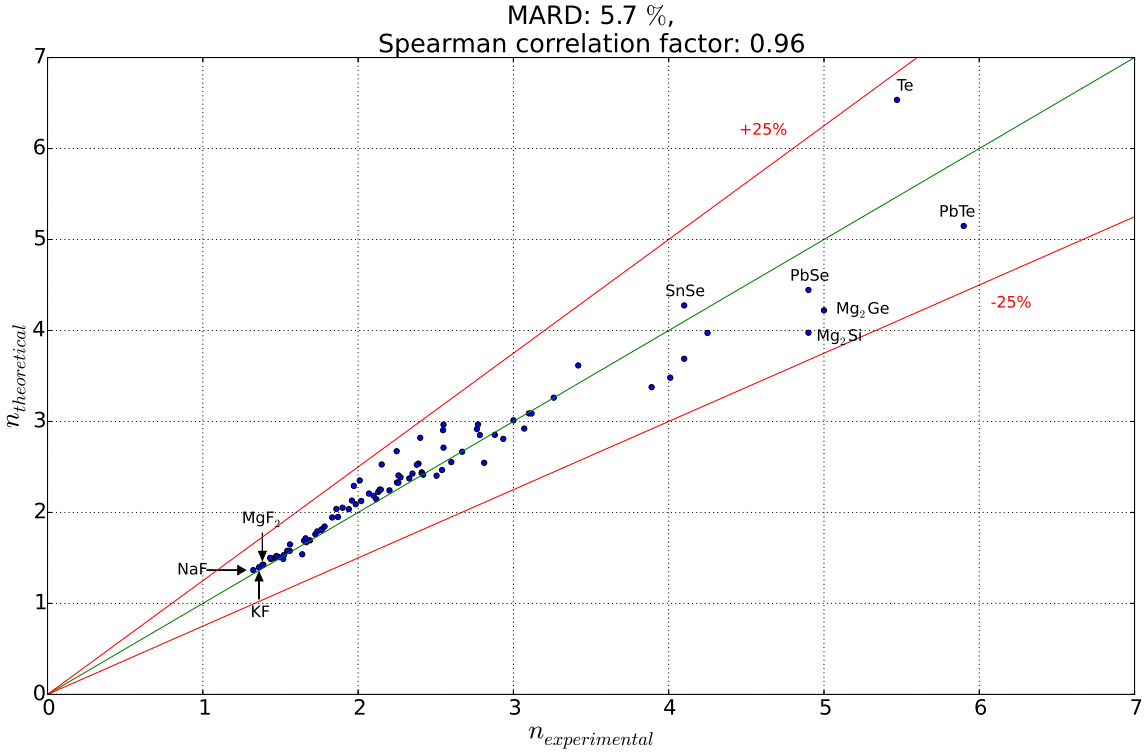

FIG. 5. Refractive index predicted by DFPT versus experimental values[40]. The refractive index was calculated as the square root of the average of the eigenvalues of the electronic dielectric tensor.

TABLE IV. Mean Absolute Relative Deviation (MARD) relative to experimental values for the refractive index predictions.

With Local Field Effects	Without Local Field Effects
5.7%	7.4%

VI. CONCLUSIONS

We have constructed as well as validated a workflow to calculate the dielectric constant in high-throughput. Our method can be used for fast screening and ranking of the dielectric constant and refractive index of materials and can serve as a first estimate before expensive calculations or experiments are carried out. Moreover, it can used to screen yet un-synthesized materials and identify potentially ferroelectric compounds. Using our numerous calculation results, we find that GGA is on average more accurate than LDA. In some cases the DFPT method leads to large deviation from experimental values - especially for the ionic part, which is due to the difficulty in correctly describing the phonon modes. This could be due to either complex structural patterns like octahedral rotation or strong phonon anharmonicity. We note that the method proposed here cannot be applied to materials with zero DFT band gap. Additionally, we found that for small band gap materials (<0.3 eV), an increase in the density of k-point mesh beyond what is suggested here will be necessary in order to obtain accurate results. Finally, we showed that it is possible to obtain consistently accurate values for the refractive index of compounds using static DFPT calculations, provided the compounds are far from optical resonance.

ACKNOWLEDGMENTS

This work was supported financially by the Volkswagen Group. Kristin Persson and Wei Chen gratefully acknowledge support from the Materials Project Center, under the Department of Energy, Basic Energy Sciences Grant No. EDCBEE. The calculations were performed using the computational resources of the National Energy Research Scientific Computing Center, which is supported under the Office of Science of the U.S. Department of Energy under Contract No. DE-AC02-05CH11231.

[1] G. Hautier, A. Jain, and S. P. Ong, *J. Mater. Sci.* **47**, 7317 (2012).
[2] A. Jain, S. P. Ong, G. Hautier, W. Chen, W. D. Richards, S. Dacek, S. Cholia, D. Gunter, D. Skinner, G. Ceder, and K. A. Persson, *APL Mat.* **1**, 011002 (2013).
[3] S. P. Ong, W. D. Richards, A. Jain, G. Hautier, M. Kocher, S. Cholia, D. Gunter, V. L. Chevrier, K. A. Persson, and G. Ceder, *Comput. Mater. Sci.* **68**, 314 (2013).
[4] S. Curtarolo, W. Setyawan, S. Wang, J. Xue, K. Yang, R. H. Taylor, L. J. Nelson, G. L. W. Hart, S. Sanvito, M. Buongiorno-Nardelli, N. Mingo, and O. Levy, *Comput. Mater. Sci.* **58**, 227 (2012).
[5] S. Curtarolo, W. Setyawan, G. L. W. Hart, M. Jahnatek, R. V. Chepulskii, R. H. Taylor, S. Wang, J. Xue, K. Yang, O. Levy, M. J. Mehl, H. T. Stokes, D. O. Demchenko, and D. Morgan, *Comput. Mater. Sci.* **58**, 218 (2012).
[6] N. E. Zein, Fiz. Tverd. Tela (Leningrad) **26**, 3024 (1984) [Sov. Phys. Solid State **26**, 1825 (1984)].
[7] S. Baroni, P. Giannozzi, and A. Testa, *Phys. Rev. Lett.* **59**, 2662 (1987).
[8] J. Zhang, Q. Zeng, A. R. Oganov, D. Dong, and Y. Liu, *Phys. Lett. A* **378**, 3549 (2014).
[9] K. Yim, Y. Yong, J. Lee, K. Lee, H.-H. Nahm, J. Yoo, C. Lee, C. S. Hwang, and S. Han, *NPG Asia Mater.* **7**, e190 (2015).
[10] J. P. Perdew and A. Zunger, *Phys. Rev. B* **23**, 5048 (1981).
[11] J. P. Perdew, K. Burke, and M. Ernzerhof, *Phys. Rev. Lett.* **77**, 3865 (1996).
[12] J. P. Perdew, K. Burke, and M. Ernzerhof, *Phys. Rev. Lett.* **78**, 1396 (1997).
[13] S. L. Dudarev, G. A. Botton, S. Y. Savrasov, C. J. Humphreys, and A. P. Sutton, *Phys. Rev. B* **57**, 1505 (1998).
[14] A. Jain, G. Hautier, C. J. Moore, S. P. Ong, C. C. Fischer, T. Mueller, K. A. Persson, and G. Ceder, *Comput. Mater. Sci.* **50**, 2295 (2011).
[15] G. Kresse and J. Hafner, *Phys. Rev. B* **47**, 558 (1993).
[16] G. Kresse and J. Hafner, *Phys. Rev. B* **49**, 14251 (1994).
[17] G. Kresse and J. Furthmüller, *Comput. Mater. Sci.* **6**, 15 (1996).
[18] G. Kresse and J. Furthmüller, *Phys. Rev. B* **54**, 11169 (1996).
[19] P. E. Blöchl, *Phys. Rev. B* **50**, 17953 (1994).
[20] G. Kresse and D. Joubert, *Phys. Rev. B* **59**, 1758 (1999).
[21] X. Gonze and C. Lee, *Phys. Rev. B* **55**, 10355 (1997).
[22] S. Baroni, S. de Gironcoli, A. Dal Corso, and P. Giannozzi, *Rev. Mod. Phys.* **73**, 515 (2001).
[23] M. Gajdoš, K. Hummer, G. Kresse, J. Furthmüller, and F. Bechstedt, *Phys. Rev. B* **73**, 045112 (2006).
[24] Z. Hashin and S. Shtrikman, *Phys. Rev.* **130**, 129 (1963).
[25] N. Marzari and D. J. Singh, *Phys. Rev. B* **62**, 12724 (2000).
[26] A. Dal Corso, S. Baroni, and R. Resta, *Phys. Rev. B* **49**, 5323 (1994).
[27] F. Kootstra, P. L. de Boeij, and J. G. Snijders, *Phys. Rev. B* **62**, 7071 (2000).
[28] V. Olevano, M. Palummo, G. Onida, and R. Del Sole, *Phys. Rev. B* **60**, 14224 (1999).
[29] W. G. Aulbur, L. Jönsson, and J. W. Wilkins, *Phys. Rev. B* **54**, 8540 (1996).
[30] Ph. Ghosez, X. Gonze, and R. W. Godby, *Phys. Rev. B* **56**, 12811 (1997).
[31] R. Resta, *Phys. Rev. Lett.* **77**, 2265 (1996).
[32] R. Resta, *Phys. Rev. Lett.* **78**, 2030 (1997).
[33] E. Cockayne and B. P. Burton, *Phys. Rev. B* **62**, 3735 (2000).
[34] E. E. Havinga, *J. Phys. Chem. Solids* **18**, 253 (1961).

[35] G. Lucovsky, J. C. Mikkelsen, W. Y. Liang, R. M. White, and R. M. Martin, *Phys. Rev. B* **14**, 1663 (1976).

[36] M. V. Nikolic, M. P. Slankamenac, N. Nikolic, D. L. Sekulic, O. S. Aleksic, M. Mitric, T. Ivetic, V. B. Pavlovic, and P. M. Nikolic, *Sci. Sinter.* **44**, 307 (2012).

[37] J. Hong, G. Catalan, J. F. Scott, and E. Artacho, *J. Phys.: Condens. Matter* **22**, 112201 (2010).

[38] M. M. Vijatović, J. D. Bobić, and B. D. Stojanović, *Sci. Sinter.* **40**, 235 (2008).

[39] H. Neumann, G. Kühn, and W. Möller, *Phys. Status Solidi B* **144**, 565 (1987).

[40] See supplemental material at [url] for a table listing calculated and experimental values.

[41] P. M. Woodward, *Acta Crystallogr. Sect. B* **53**, 32 (1997).

[42] J. M. Rondinelli and N. A. Spaldin, *Phys. Rev. B* **82**, 113402 (2010).

[43] L. He, F. Liu, G. Hautier, M. J. T. Oliveira, M. A. L. Marques, F. D. Vila, J. J. Rehr, G.-M. Rignanese, and A. Zhou, *Phys. Rev. B* **89**, 064305 (2014).

[44] W. Martienssen and H. Warlimont, *Springer handbook of condensed matter and materials data*, (Springer Science & Business Media, 2006).

[45] K. F. Young and H. P. R. Frederikse, *J. Phys. Chem. Ref. Data* **2**, 313 (1973).

[46] M. Schulz, O. Madelung and U. Rössler, Springer materials, `http://materials.springer.com/lb/docs/sm_lbs_978-3-540-31360-1_559`, [Online; accessed 22 June 2015].

[47] M. Schulz, O. Madelung and U. Rössler, Springer materials, `http://materials.springer.com/lb/docs/sm_lbs_978-3-540-31360-1_571`, [Online; accessed 22 June 2015].

[48] M. Schulz, O. Madelung and U. Rössler, Springer materials, `http://materials.springer.com/lb/docs/sm_lbs_978-3-540-31360-1_588`, [Online; accessed 22 June 2015].

[49] M. Schulz, O. Madelung and U. Rössler, Springer materials, `http://materials.springer.com/lb/docs/sm_lbs_978-3-540-31360-1_881`, [Online; accessed 22 June 2015].

[50] M. Schulz, O. Madelung and U. Rössler, Springer materials, `http://materials.springer.com/lb/docs/sm_lbs_978-3-540-31360-1_895`, [Online; accessed 22 June 2015].

[51] M. Schulz, O. Madelung and U. Rössler, Springer materials, `http://materials.springer.com/lb/docs/sm_lbs_978-3-540-31360-1_719`, [Online; accessed 22 June 2015].

[52] Ph. Ghosez, X. Gonze, and J.-P. Michenaud, *Ferroelectrics* **164**, 113 (1995).

[53] C. Lasota, C.-Z. Wang, R. Yu, and H. Krakauer, *Ferroelectrics* **194**, 109 (1997).

[54] U. V. Waghmare and K. M. Rabe, In *Materials Fundamentals of Gate Dielectrics*, (p. 215, Springer, 2005).

[55] M.-H. Du and D. J. Singh, *Phys. Rev. B* **81**, 144114 (2010).

[56] Y. Zhang, X. Ke, C. Chen, J. Yang, and P. R. C. Kent, *Phys. Rev. B* **80**, 024304 (2009).

[57] R. A. Cowley, *Philos. Mag.* **11**, 673 (1965).

[58] J. Shanker and R. Sundaraj, *Phys. Status Solidi B* **115**, 67 (1983).

[59] O. Delaire, J. Ma, K. Marty, A. F. May, M. A. McGuire, M.-H. Du, D. J. Singh, A. Podlesnyak, G. Ehlers, M. D. Lumsden and B. C. Sales, *Nat. Mater.* **10**, 614 (2011).

[60] A. D. Bruce and R. A. Cowley, *J. Phys. C* **6**, 2422 (1973).

[61] B. Szigeti, *Proc. R. Soc. A* **252**, 217 (1959).

[62] K. A. Müller, Y. Luspin, J. L. Servoin, and F. Gervais, *J. Phys. Lett. Paris* **43**, 537 (1982).

[63] E. C. Fieller, H. O. Hartley, and E. S. Pearson, Tests for Rank Correlation Coefficients. I, *Biometrika* **44**, 470 (1957).